SARS-CoV-2 infection paralyzes cytotoxic and metabolic functions of the immune cells

Yogesh Singh[1,2,6*,#], Christoph Trautwein[3*], Rolf Fendel[4*], Naomi Krickeberg[4], Georgy Berezhnoy[3], Rosi Bissinger[5], Stephan Ossowski[1,2], Madhuri S. Salker[6], Nicolas Casadei[1,2], Olaf Riess[1,2#] and the Deutsche COVID-19 OMICS Initiative (DeCOI)

[1]Institute of Medical Genetics and Applied Genomics, University of Tübingen, Calwerstrasse 7, 72076, Tübingen, Germany
[2]NGS Competence Center Tübingen (NCCT), University of Tübingen, Calwerstrasse 7, 72076 Tübingen, Germany
[3]Werner Siemens Imaging Center, University of Tübingen, Röntgenweg 13, 72076, Tübingen, Germany
[4]Institute of Tropical Medicine, University Hospital of Tübingen, Tübingen, Wilhelmstrasse 27, 72076, Tübingen, Germany
[5]Department of Internal Medicine, Division of Endocrinology, Diabetology and Nephrology, University Hospital of Tübingen, Germany
[6]Research Institute of Women's Health, University of Tübingen, Calwerstrasse 7/6, 72076, Tübingen, Germany
*Equal contributions
Correspondence
Dr Yogesh Singh or Prof Olaf Riess
Institute of Medical Genetics and Applied Genomics, Tübingen University
Calwerstraße 7, 72076, Tübingen, Germany
Phone: 0049 7071 29 72257/78264 Fax: 0049 7071 29 25355
Email: yogesh.singh@med.uni-tuebingen.de or olaf.riess@med.uni.tuebingen.de

Abstract:

The SARS-CoV-2 virus is the causative agent of the global COVID-19 infectious disease outbreak, which can lead to acute respiratory distress syndrome (ARDS). However, it is still unclear how the virus interferes with immune cell and metabolic functions in the human body. In this study, we investigated the immune response in acute or convalescent COVID19 patients. We characterized the peripheral blood mononuclear cells (PBMCs) using flow cytometry and found that $CD8^+$ T cells were significantly subsided in moderate COVID-19 and convalescent patients. Furthermore, characterization of $CD8^+$ T cells suggested that patients with a mild and moderate course of the COVID-19 disease and convalescent patients have significantly diminished expression of both perforin and granzyme A in $CD8^+$ T cells. Using ^{1}H-NMR spectroscopy, we characterized the metabolic status of their autologous PBMCs. We found that fructose, lactate and taurine levels were elevated in infected (mild and moderate) patients compared with control and convalescent patients. Glucose, glutamate, formate and acetate levels were attenuated in COVID-19 (mild and moderate) patients. In summary, our report suggests that SARS-CoV-2 infection leads to disrupted $CD8^+$ T cytotoxic functions and changes the overall metabolic functions of immune cells.

Key words: COVID-19, $CD8^+$ T cells, Granzyme A, Perforin, Metabolites, ^{1}H-NMR, Flow cytometry

Short title: Defective immune-metabolic functions in COVID-19 patient

Introduction:

The first cases of severe acute respiratory coronavirus-2 (SARS-CoV-2) infection appeared in December 2019, in Wuhan, China[1]. This zoonotic virus has infected by now more than 127.8 million people (30.03.2021) and has resulted more than 2.78 million[2,3] death worldwide. The containment of the pandemic is challenging and is still growing with roughly 200,000 or more new infections being reported daily since July 2020[2,3]. There is an urgent need for a better understanding of immunopathology, as SARS-CoV-2 has become the leading cause of morbidity (long COVID syndrome) and mortality in many countries.

Coronaviruses (CoV) are a large family of viruses that can cause illnesses such as the common cold and seasonal influenza[4]. Pathologically, SARS-CoV-2 typically infects via angiotensin-converting enzyme 2 (ACE2)-expressing nasal epithelial cells in the upper respiratory tract and type II alveolar epithelial cells in patients exhibiting pneumonitis[1,5]. The most severe disease courses led frequently to death but, not exclusively in older patients with and without risk conditions. The primary symptoms of SARS-CoV-2 infections are fatigue, fever, sore throat, dry cough, loss of smell and taste within 5-21 days of incubation of the virus[6-9]. COVID-19 symptoms are heterogeneous and range from asymptomatic to mild, moderate, and severe pathological symptoms, presenting with or without pneumonia[10,11]. However, most infected people develop mild to moderate illness and recover without hospitalization[12,13]. High serum levels of IL-6, IL-8, IL-10, TNF-α cytokines and an immune hyper-responsiveness referred to as a 'cytokine storm' is connected with poor clinical outcome[14,15]. Predominantly, older COVID-19 patients can develop acute severe respiratory distress syndrome (ARDS) due to a cytokine storm which is a life-threatening situation, requiring ventilation and intensive care support[16-20].

Several break-through discoveries have extended our understanding as to how the virus takes advantage of the host and modulates immunity[12,19,21-25]. Recovered COVID-19 patients have an increased number of antibody-secreting cells and activated $CD4^+$ and $CD8^+$ T cells. Further, Immunoglobulin M (IgM) and SARS-CoV-2 reactive IgG antibodies were also detected in blood before full symptomatic recovery[26-28]. Most severely affected COVID-19 patients had a lower T cell but elevated B cell counts when compared with healthy controls[13,14,29,30]. Interestingly, patients with mild symptoms were also shown to have increased T and B cells compared with severely affected patients[26,29-31]. There could be several reasons for different disease outcomes including an over-activated innate or hyper-activated adaptive immune response leading to cytokine storms and resulting in severe injury to the lungs[10,13,25,32]. Despite several ongoing efforts, the immunological mechanisms of the host-pathogen interaction are not well understood[33].

There is an intricate balance between the metabolic state of immune cells and generation of a robust immune response[19,34-37]. $CD8^+$ T cells require energy to proliferate and accomplish their effective functions[38]. Most propagating cells such as lymphocytes utilize the most abundant energy substrates including, glucose, lipids, and amino acids[39]. In response to SARS-CoV-2 and other virus infections, $CD8^+$ T cells play a pivotal role in profound growth and proliferation to generate their effective functional cells which can produce copious amounts of effector molecules such as cytokines and cytotoxic granules[30,38-40]. An activated immune system is coupled with a change in metabolic reprogramming to produce enough energy needed during (viral) infection[38,39]. Proliferating T cells ferment glucose to lactate even

in the presence of oxygen to meet high energy demands[34,37-39]. Furthermore, glucose and glutamine are involved in the hexosamine biosynthetic pathway, which regulates the production of uridine diphosphate N-acetyl glucosamine necessary for T cell clonal expansion and function[41]. The synthesis of lactate intracellularly is crucial for T cells to have an increased glycolytic flux[38].

Peripheral blood mononuclear cells (PBMCs) can be analyzed to measure the physiological dysfunctionality of an individual and can serve as a biomarker[42]. Consequently, the metabolic status of lymphocytes could help to predict disease severity or to select the optimal therapeutic intervention to boost the immune function during infection. Generally, most of the metabolism-related functions in PBMCs during SARS-CoV-2 infections were inferred based on transcriptomics analysis[34,43] and no functional data (biochemical level) have been presented. Therefore, understanding the kinetics of the adaptive immune response as well as the metabolic functions during SARS-CoV-2 infection will help to elucidate the host immune response to SARS-CoV-2 infection. In this study, using flow cytometry and proton nuclear magnetic resonance (^{1}H-NMR) spectroscopy, we characterized the PBMCs from SARS-CoV-2 infected and convalescent patients for their immunophenotypic and metabolic functions.

Results:

Characteristics of study participants

PBMCs were isolated and cryopreserved from blood samples obtained from COVID-19 patients suffering from mild ('Mild (outpatient)') or moderate/severe ('Moderate (inpatient)') disease or were already recovered ('Convalescent') and from healthy controls ('HC'). Classification of disease severity for this analysis was based on the requirement of hospitalization. Patients with mild COVID-19 were recruited within three days after confirmation of infection by RT-qPCR. From moderate to severe COVID-19 patient blood samples were collected one week after their hospital admittance. The moderate patients were admitted to the hospital requiring medical care; however, they did not need ventilation or O_2 supply. Recovered patients were included based on a positive SARS-CoV-2 antibody testing. Study participant characteristics are described in Table 1.

Table 1: Patient demographics

No	COVID-19 status	Blood sampling	COVID-19 severity	Sex	Age
1	Outpatient (mild)	Day1	mild	F	21
2	Outpatient (mild)	Day1	mild	M	59
3	Outpatient (mild)	Day1	mild	F	40
4	Inpatient (moderate)	Day7	Moderate	M	57
5	Inpatient (moderate)	Day7	Moderate	M	47
6	Inpatient (moderate)	Day7	Moderate	F	78
7	Convalescent (Sero +ve)	Convalescent	Recovered, healthy	F	50
8	Convalescent	Convalescent	Recovered, healthy	F	24

	(Sero +ve)				
9	Convalescent (Sero +ve)	Convalescent	Recovered, healthy	M	50
10	Convalescent (Sero +ve)	Convalescent	Recovered, healthy	F	51
11	HC1	-	None	F	36
12	HC2	-	None	M	60
13	HC3	-	None	M	40
14	HC4	-	None	M	37
15	HC5	-	None	M	47

Immunophenotyping of COVID-19 mild, moderate and convalescent COVID-19 patients

To compare the number of lymphocytes and monocytes amongst the four study groups, PBMCs were stained and analysed by flow cytometry. Based on live-cell percentage count (gating strategy; Suppl. Fig. 1a), both, lymphocytes and monocytes were not significantly different among mild, moderate and convalescent COVID-19 patients compared with HC (Suppl. Fig. 1b-d).

Increased inflammatory monocytes and reduced NK cells in moderate COVID-19 patients

Monocytes were further classified into classical, non-classical and intermediate based on the expression of CD16 and/or CD14 and were gated as described earlier[44] (Suppl. Fig. 1a). We found that $CD16^{+}CD14^{-}$ patrolling (non-classical) monocytes were significantly increased (p=0.0004) in percentage in moderate patients compared to HC, whereas this number is decreased again significantly compared with convalescent patients (p=0.001) (Fig. 1a). The percentage of $CD16^{+}CD14^{-}$ (non-classical) monocytes was also significantly increased (p=0.006) in moderate patients compared with mild patients (Fig. 1a Panel I; left). Interestingly, $CD16^{+}CD14^{+}$ pro-inflammatory monocytes (intermediate) were again significantly increased in mild (p=0.03) and moderate (p=0.002) compared with HC as well as between moderate and convalescent (p=0.005) (Fig. 1a panel II; middle). Furthermore, we observed a significantly reduced percentage of $CD14^{+}CD16^{-}$ phagocytic monocytes (classical) in moderate compared with mild (p=0.004), HC (p<0.0002) and convalescent (p=0.0007) patients (Fig. 1a Panel III; right). Based on the results above using classical 2D flow cytometry analysis, we observed a major difference between HC *vs* mild or with moderate COVID-19 patient samples, therefore, we concatenated three groups together (equal number of cells from each sample; HC, mild and moderate) to identify the visual clustering of monocytes using Uniform Manifold Approximation and Projection (UMAP) for dimension reduction algorithm[45] (Suppl. Fig. 2). Based on UMAP dimension reduction analysis (data-driven and gated cells), we observed a clear difference in the different subsets of monocytes between all three groups (Suppl. Fig. 2c, d & Fig. 1b). We observed that moderate COVID-19 patients mostly cluster in non-classical and partially in intermediate monocyte regions compared to HC, whilst mild COVID-19 patients cluster in all non-classical, intermediate and classical monocytes regions (Fig. 1b; right). We then explored the lymphoid cells compartment for NK cells ($CD56^{+}CD8^{+}CD3^{-}CD19^{-}$). We found that moderate patients were significantly different from HC (p=0.04). There was also a

169 tendency of a decrease in NK cells in mild patients compared with HC (p=0.07), although, not
170 reaching statistical significance (Fig. 1c).
171
172 *Dynamics of B and T cells in mild, moderate and convalescent patients*
173
174 Both T and B cells are indispensable for the immune response against viral infections including
175 SARS-CoV-2. Firstly, we compared the number of B cells amongst the study groups, which
176 give rise to virus-specific antibodies (see the gating strategy in Suppl. Fig. 1a). The $CD19^{+}CD3^{-}$
177 cells (B cells) were significantly increased in mild (p=0.008; fold change x1.7) and moderate
178 (p=0.0008; fold change x1.9) patients compared with HC (Fig. 2a). Whilst, B cells were
179 significantly decreased in moderate compared to convalescent (p=0.04) patients (Fig. 2a).
180 Comparing $CD3^{+}CD19^{-}$ lymphocytes among the different patient groups we observed no
181 significant difference. Moreover, $CD3^{+}$ cells were analysed for the $CD4^{+}$ and $CD8^{+}$ T cell
182 compartment. There was a tendency of increased $CD4^{+}$ T cells for mild, moderate, and
183 convalescent patients compared to HC, but no significant difference was observed among any
184 of the groups. $CD8^{+}$ T cells were significantly different between HC compared to moderate
185 (p=0.04) or convalescent (p=0.04) patients (Fig. 2b). Finally, we characterized
186 $CD4^{+}FOXP3^{+}CD45R^{-}$ regulatory T cells (Tregs), however, no significant difference was
187 observed among the different groups (Suppl. Fig. 3).
188
189 *Impaired activation and defective cytotoxic functions of $CD8^{+}$ T cells*
190
191 We found that the percentage of $CD8^{+}$ T cells were decreased in mild and convalescent
192 patients compared to HC. Thus, we explored the activation status of $CD8^{+}$ T cells based on
193 HLA-DR expression. We found that $CD8^{+}$ T cell activation status in all three groups of infected
194 patients was significantly different from HC (mild p=0.01, moderate p=0.01, and convalescent
195 p=0.01, Fig. 3a). We characterized the cytotoxic potential of $CD8^{+}$ T cells based on granzyme
196 A and perforin levels and found that there was a tendency of decreased granzyme A
197 expression in mild, moderate and convalescent patients compared with HC (Fig. 3b), however,
198 it did not reach significance. Perforin was significantly decreased in convalescent (p=0.02)
199 patients compared with HC (Fig. 3b), although mild patients also had reduced levels (p=0.07),
200 it did not reach statistical significance. Furthermore, we studied the expression of CD38, a
201 marker of immune cell activation, which was significantly upregulated in convalescent patients
202 compared with HC (p=0.04) (Fig. 4a). Similarly, convalescent patients had significantly
203 increased numbers of $PD\text{-}1^{+}$ $CD38^{+}$ cytotoxic $CD8^{+}$ T cells compared with HC (p=0.006),
204 moderate (p=0.005) and mild (p=0.002), which reflects the exhaustion and non-
205 responsiveness (anergy) of $CD8^{+}$ T cells (Fig. 4b). Overall, our data suggested that $CD8^{+}$ T
206 cells have reduced activation, diminished expression of cytotoxic molecules such as perforin
207 and granzyme A and have a severely exhausted phenotype.
208
209 *Dynamics of metabolites production in the mild, moderate and convalescent patient*
210
211 To establish a putative link between the metabolic state of immune cells and the impaired
212 immune response, PBMCs from all patient groups were subjected to ^{1}H-NMR spectroscopy
213 analysis. We identified and quantified a total of 18 metabolites (Fig. 5a). Hereby, unsupervised
214 Principal Component Analysis (PCA) showed that spectral data from mild and moderate
215 patients formed overlapping clusters. However, HC and convalescent patients clustered
216 together (Fig. 5b), indicating a strong difference in metabolite levels between an infectious

217 state compared to healthy or recovered groups. Statistical analysis of the four different groups
218 revealed that 15 metabolites showed p-values < 0.05, with the highest significance for
219 metabolites related to energy metabolism (Fig. 5c, Suppl. Fig. 3 & Table 2). The data indicate
220 that during infection, there is a strong consumption (reflecting reduced levels) of glucose,
221 acetate and formate, whilst lactate levels are increased. Furthermore, we also found very high
222 levels of fructose in PBMCs from mild patients, medium concentrations in moderate and, low
223 levels in HC and convalescent patients (Fig. 5c). Furthermore, glutamate was almost
224 abolished in mild and moderate patients, potentially as a consequence of enhanced
225 production of α-ketoglutarate in the TCA cycle in PBMCs *via* glutamate dehydrogenase (Fig.
226 5c). Levels of other amino acids such as glycine and isoleucine were low in mild and moderate
227 patients compared with HC, while creatine and alanine were high in mild patient and moderate
228 patient respectively (Fig. 5c).
229
230 **Table 2: Summary of metabolites dysregulated in PBMCs**
231

No	Metabolites	HC	Mild	Moderate	Convalescent
1	Glucose	↑↑	↓↓	↓↓	↑↑
2	Formate	↑↑	↓↓↓	↓↓	↑↑
3	Acetate	↑	↓↓	↓	↑
4	Lactate	↓↓	↑↑	↑↑	↓↓
5	Fructose	↓	↑↑	↑	↓
6	Glutamate	↑	↓	↓	↑
7	Citrate	↓	↑↑	↑	↓
8	Taurine	↓↓	-	↑↑	↓
9	Creatine	↓	↑	-	-
10	Alanine	↓	-	↑↑	↓
11	Glycine	↑	↓	↓	-
12	Isoleucine	-	↓↓	↓	↑

232
233 To find an association between different metabolites, we applied the variable importance of
234 projection (VIP) score. We found that formate and glucose had the highest score compared to
235 other metabolites (Fig. 6A). To determine if additional metabolites are positively associated
236 with changes in glucose, lactate and fructose, we performed a pattern hunter analysis for all
237 metabolites. We found that high glucose levels correlated with high formate, acetate and
238 glutamate and low lactate and fructose (Fig. 6b), indicating enhanced glycolysis and TCA cycle
239 in PBMCs. Similarly, fructose, which is entered *via* fructose-1-phosphate and
240 dihydroxyacetone phosphate (DAP) into the glycolysis, is correlated positively with lactate and
241 citrate and a decrease in acetate and formate, respectively (Fig. 6b). Interestingly, levels of
242 the ROS scavenger taurine are only positively correlated with lactate and fructose, but not
243 glucose (Fig. 6).
244
245 **Discussion:**
246
247 SARS-CoV-2 infections are an intense and rapidly evolving area of research due to the
248 ongoing global pandemic[14,25]. In this study, we used flow cytometry and ^{1}H-NMR to decipher
249 the cell proportions and functional state of immune cells (PBMCs) in mild, moderate and
250 convalescent COVID-19 patients compared to HC. Recent reports from COVID-19 patients

251 suggested that mild and severe patient had lymphopenia[11,46-48]. Here, we found that the
252 myeloid cell compartment in PBMCs based on CD16 and CD14 markers suggested that the
253 percentage of non-classical and intermediate monocytes were increased during an active mild
254 or moderate SARS-CoV-2 infection, once infections are cleared the monocyte percentage
255 numbers return to normal. These results are in accordance with some of the recently published
256 studies[49-51].
257
258 In our cohort, specifically $CD56^+CD8^+$NK cells were decreased during active SARS-CoV-2
259 viral infections (moderate), while during recovery the numbers were comparable to HC as
260 reported by others[52]. Similarly, another recent study supports our finding by showing the
261 decrease in the number of NK cell subsets in COVID-19 patients, with no change in $CD56^{bright}$
262 or $CD56^{dim}$ cells[53]. Furthermore, based on single-cell RNA-sequencing data, a reduced
263 number of NK cells was reported in the recovered COVID-19 patients[48]. Thus, altogether, it
264 appears that $CD56^+$NK cells and their subsets could have an important function during the
265 ongoing and clearance of SARS-CoV-2 infections. However, further validation studies are
266 warranted using different *in vivo* model systems with appropriate control groups to pinpoint
267 the exact role of different NK cell subsets in SARS-CoV-2 infection. $CD19^+$ B lymphocytes
268 were increased during infection and remain slightly higher than HC, thus reflecting the
269 antibody response against the SARS-CoV-2 virus. Thus, our data suggest that these patients
270 were able to generate SARS-CoV-2 specific B cells, this needs further scientific validation.
271
272 A major difference was found in the T lymphocytes compartment. $CD8^+$ T cells were
273 significantly decreased in moderate and convalescent patients as reported earlier[52]. Thus, it
274 appears that during viral infection non-virus specific $CD8^+$ T cells undergo apoptosis, whilst
275 the viral-specific surviving $CD8^+$ T cells are clonally expanded but appeared to have lost their
276 effector functions[54]. To confirm this, we first measured the activation status of $CD8^+$ T cells
277 and found that $CD8^+$ T cells appeared to be less activated based on their HLA-DR activation
278 marker[26]. Further, $CD8^+$ T cells were examined for additional activation marker CD38, which
279 is involved in cell adhesion, signal transduction and calcium signalling[55], was found to be
280 upregulated in convalescent patients but not during active infection. These $CD38^+CD8^+$ T cells
281 also expressed higher levels of PD-1, which is an immune checkpoint and marker of
282 exhaustion[24,30,56-58]. PD-1 further guards against autoimmunity promote apoptosis of antigen-
283 specific T cells and promotes self-tolerance by suppressing T cell inflammatory activity[59].
284 Thus, viral infection leaves convalescent patients with exhausted phenotypes. We uncovered
285 that although there was not a significant change in the numbers of Tregs in COVID-19 patients,
286 there was a trend towards elevated levels of Tregs in COVID-19 patients and rescued Tregs
287 in convalescent patients, in agreement with the previous studies[56].
288
289 A key finding of our study was the surprising observation that granzyme A and perforin
290 secreting $CD8^+$ T cells were significantly reduced in convalescent patients. These results are
291 in agreement with the recent single-cell transcriptomics analysis which suggests that
292 granzyme B and perforin-1 transcripts were also decreased in convalescent COVID-19
293 patients compared with moderate or severe illness[60]. In contrast to our results, in young
294 patients, granzyme A or B and perforin levels were increased in mild and moderate cases.
295 Conversely, in elderly COVID-19 patients, there was a reduced expression of granzyme A and
296 perforin[61]. Another study suggested that decreased perforin and granzyme A levels in $CD4^+$ T
297 cells, $CD8^+$ T cell and NK cells is associated with severely afflicted COVID-19 patients[62].
298 Furthermore, single-cell transcriptomics analysis of SARS-CoV-2 reactive $CD8^+$ T cells in

exhausted and non-exhausted subsets were analyzed[63]. These exhausted $CD8^+$ T cells were increased in frequency and displayed lesser cytotoxicity and inflammation features in mild COVID-19 patients compared to severe patients[63]. A genetic study performed on two cases highlights the importance of the perforin gene variant A91V which results in the rapid demise in young COVID-19 patients[64]. The possible implication of our finding is that convalescent patients, specifically including cancer patients under treatment, could be susceptible to future opportunistic infections with other viruses including different variants of SARS-CoV-2. However, further, a large cohort study is warranted to understand the potential functions of these molecules (granzyme or perforin) in protection or susceptibility against the COVID-19 infection at gene and function levels.

To date, the general metabolic physiology of PBMCs is not well defined in the literature. However, it is clear now that PBMCs are dependent on circulating nutrients and hormones in the blood[65]. A defective immune response in COVID-19 patients prompted us to investigate the metabolic functions of these immune cells. Our metabolomics data indeed shows that PBMCs from actively infected patients have a distinct metabolic profile from convalescent or healthy individuals. The most notable difference we observed was for metabolites from the glycolysis and oxidative phosphorylation (TCA cycle) pathway, which is per recently published transcriptome data for PBMCs[39,43]. Metabolites such as glucose, formate, acetate and choline were also reduced in PBMCs in infected patients whereas, HC and convalescent patients had a normal profile. Accordingly, the glycolytic pathway end products such as lactate were higher in active mild and moderate COVID-19 patients compared with HC and convalescent individuals. Therefore, our data suggest that PBMCs (which constitute a major fraction of T lymphoid cells: 70- 80%) may have modulated their metabolic functions, particularly favouring the oxidative phosphorylation pathway over the glycolytic pathway, to meet the high demands of energy needed to combat the ongoing viral infection.

A recent report suggested that elevated glucose levels enhance SARS-CoV-2 replication and cytokine expression in monocytes and glycolysis sustains the viral-induced monocyte response[66]. Recently, it was emphasized that glucose consumption in PBMCs during COVID-19 disease could be also a read-out of cytokine storms[34]. Further, a higher abundance of citrate in PBMCs suggested that perhaps T cells could use the oxidative phosphorylation pathway for energy consumption to endure the infection, as recent transcriptomic data also suggested that higher expression of genes related to oxidative phosphorylation both in peripheral mononuclear leukocytes and bronchoalveolar lavage fluid (BALF) could play a crucial role in increased mitochondrial activity during SARS-CoV-2 infection[34].

Another remarkable finding of our study was the increase of fructose levels in PBMCs during the course of infection. Previous findings suggested that fructose is involved in the inflammatory pathways for the production of IL-1β and IL-6 production[67]. Thus, it is conceivable that the immune cells (most probably monocytes) could be triggered by higher fructose and simultaneously induce inflammation and IFN-γ production by T cells[67]. These findings correlate with recent transcriptomic studies on the BALF from infected COVID-19 patients and plasma of COVID-19 patients that also identified changes in fructose metabolism[34,68].

Several amino acids are involved in anti-inflammatory effects, especially arginine, glutamine and glycine appeared to improve lung damage induced by infections[69]. Administration of

347 glutamine reduced the inflammatory cytokines, whereas arginine or glycine reduced IL-6 and
348 CXCL-1 expression in the alveolar epithelium[70]. Additionally, glutamine is an important
349 signalling molecule involved in activating mammalian target of rapamycin (mTOR) signalling
350 which is critical for immune cell activity and inhibiting catabolic functions such as protein
351 degradation and apoptosis[71]. In our study, we found a reduced abundance of glutamate and
352 glycine in PBMCs during the mild and moderate COVID-19 patients. Reduced glucose and
353 glutamine are involved in the hexosamine biosynthetic pathway and could be responsible for
354 poor T cell clonal expansion and function[41]. The exact molecular mechanism of individual
355 amino acids is a complex phenomenon and currently unclear. However, at least in theory,
356 supplementation of glutamine and glycine could be beneficial for COVID-19 patients.
357
358 We finally observed a reduction of granzyme A and perforin levels in $CD8^+$ T cells and detected
359 the ambient level of antioxidant amino acid taurine in the convalescent patients, which could
360 be involved in the modulation of cytotoxic functions of $CD8^+$ T cells. Both granzyme A and
361 perforin are involved in ROS production and taurine serves as ROS scavenger[72,73]. Thus,
362 decreased granzyme A and perforin could be implicated in reduced ROS production for the
363 impaired effectiveness of $CD8^+$ T cells in either convalescent patients or COVID-19 patients.
364 This should be the case, as taurine levels are generally increased during active infection in
365 mild/moderate patients compared to healthy controls and are not specifically decreasing due
366 to granzyme A and perforin lacking ROS activity in COVID-19 patients. However, this finding
367 needs further investigation to validate this hypothesis as it is unclear how ROS and taurine act
368 together to affect the cytotoxic functions of immune $CD8^+$ T cells. In summary, the
369 metabolomics data generated in this study provides first and crucial insights into the complex
370 metabolic changes of PBMCs during SARS-CoV-2 infections, warranting further future in-
371 depth investigation.
372
373 **Conclusions:**
374 Using immunophenotyping and metabolomics approaches we detected significant changes in
375 PBMC samples of mildly and moderately affected COVID-19 as well as convalescent patients
376 compared with healthy controls. The reduced percentage of NK cells in both mild and
377 moderate patient groups corresponded with the clustering of PBMCs metabolite levels in the
378 principal component analysis distinct from the cluster formed by healthy and convalescent
379 individuals. The dramatically changed metabolic activity and pathways, such as glycolysis and
380 TCA cycle, might not only lead to a vulnerability of COVID-19 patients to subsequent infections
381 but can also offer insights into how PBMCs could be manipulated towards a better survival
382 and personalized treatment of moderate and severe COVID-19 patients.
383
384 **Limitation of the study:**
385 The current study is performed from the samples obtained during the first wave of infections
386 and suffers from the limited number of patients used in the study. The use of appropriate
387 controls such as influenza viral infection would have been useful for a more generalized
388 conclusion. Therefore, results obtained in future studies might differ from subsequent waves
389 of infections in new patient cohorts. Further, the novel SARS-CoV-2 variants or vaccine
390 candidates might promote alternative host immune evasion strategies to infect the host, thus,
391 eliciting a different immune response. Nonetheless, this study certainly highlights the
392 importance of distinct cell types as well as the crucial function of cell metabolism during SARS-
393 CoV-2 viral infection and even after recovery.
394

Materials and Methods:

Ethics statement

The study protocols were approved by the University of Tübingen, Germany Human Research Ethics Committee (TÜCOV: 256/2020BO2 (convalescent study), COMIHY: (225/2020AMG1) (outpatient study)-COMIHY, EUDRA-CT: 2020-001512-26, ClinicalTrials.gov ID: NCT04340544, and COV-HCQ: (190//2020AMG1) (inpatient study)-COV-HCQ, EUDRA-CT: 2020-001224-33, ClinicalTrials.gov ID: NCT04342221, 556/2018BO2) and all associated procedures were carried out in accordance with approval guidelines. All participants provided written informed consent in accordance with the Declaration of Helsinki.

Study participants

SARS-CoV-2 positive patients were used for this study and no other virus species were analysed in this study (COMIHY and COV-HCQ). Blood was collected from COVID-19 patients enrolled into two different prospective randomized, placebo-controlled, double-blind clinical trials evaluating the safety and efficacy of hydroxychloroquine in COVID-19 outpatients (COMIHIY) and hospitalized patients (COV-HCQ). We analysed subsets of these study cohort and used outpatient (n=3; COMIHY) which came to a specified outpatient ward at the Institute of Tropical Medicine with mild symptoms and blood was taken and usually defined as D1 outpatients. Inpatients (n=3; COV-HCQ), blood was taken after 7-9 days after study inclusion defined as D7. These patients had moderate symptoms needing hospital care, however not being transferred to the intensive care unit in the hospital. Furthermore, convalescent COVID-19 patients (n=4) were defined as positive for serum antibody reactive to SARS-CoV-2 and blood was taken when they visited the Institute of Tropical Medicine for testing of antibody levels. Amongst this cohort, 3 persons reported mild fever for 10-11 days and 1 individual reported no fever but found positive for SARS-CoV-2 antibodies. Blood from healthy controls (n=5) was obtained from the hospital blood bank.

Flow cytometry and UMAP data analysis

PBMCs were isolated by the standard Ficoll method[74]. A total of 1-2 x10^6 PBMCs per participants were used for three FACS panels (Table 2). In brief, firstly, to distinguish between live from dead, the cells were incubated with LIVE/DEAD Fixable Infra-Red Dead stain (Thermofisher) for 15 minutes at room temperature (RT) into 1:40 diluted dye in DPBS. Subsequently, after LIVE/DEAD staining, cells were stained with surface markers in DPBS (Sigma) with Super Bright stain Buffer (Thermofisher) for 30 minutes at RT. After surface staining cells were also stained for intracellular (IC) markers. Before IC staining, cells were fixed for 30-45 minutes and permeabilized for 5 minutes followed by IC antibody incubation for additional 30 minutes at RT. Cells were washed and resuspended in DPBS containing 2%FBS. Fixing of cells was performed irrespective of whether the panel was used for IC staining or not to prevent the possible contamination during the acquisition of the samples. All the staining procedures were performed in the dark to avoid the photo-bleaching of dyes. For each sample, 200,000 cells were acquired using BD LSRFortessa (core facility) equipped with 4 lasers (violet, blue and yellow-green and Red). Data were analysed using Flow Jo (Tree Star) and fluorescence minus one controls (FMO) were used for setting up the arbitrary gates

444 for the major cell markers. Furthermore, UMAP dimensional reduction analysis was performed
445 using UMAP plug-in[45] in Flowjo software using default setting except for minimum distance
446 (0.2 instead of 0.5) and population (n=15) as advised by a plug-in. First, dead/debris was
447 removed by gating (FSC-A vs SSC-A; linear scale) then using FSC-A vs FSC-W, we focussed
448 on singlets. The singlets were again gated for live and dead discrimination. An equal number
449 of live cells from each sample (HC, mild and moderate) were concatenated and exported as
450 a single FCS file. This FSC file was subjected to UMAP analysis, each cell population was
451 either monocytes or lymphocytes were again subject to subsequent UMAP analysis for
452 clustering of specific sub-populations. Based on gating or antibodies-stained cells (data
453 driven) analysis was performed and summarized in Suppl. Fig. 2.
454
455 **Table 2: Antibodies and other reagents used for Flow cytometry**
456

No.	Product Name	Clone	Fluorochrome	Product ID	Company
		NK cells and Monocytes (Panel 1)			
1	CD3	UCHT1	eFluor 450	48-0038-42	Thermofisher
2	CD4	SK3	SuperBright 600	63-0047-42	Thermofisher
3	CD8a	SK1	PerCP-eFluor 710	46-0087-42	Thermofisher
4	CD19	HIB19	eFluor 506	69-0199-42	Thermofisher
5	CD45-RA	HI100	PE-Cy7	25-0458-42	Thermofisher
6	HLA-DR	L243	Alexa Fluor647	A51010	Thermofisher
7	CD38	HIT2	PE-eFluor610	61-0389-42	Thermofisher
8	CD56	MEM188	PE	MA119638	Thermofisher
9	CD16	3G8	Super Bright702	67-0166-42	Thermofisher
10	CD14	61D3	Alexa Fluor700	56-0149-42	Thermofisher
11	Foxp3 (IC)	PCH101	FITC	11-4776-42	Thermofisher
		CD8 exhaustion, T helper follicular cells (Tfh) and antibody-secreting cell (ASC) (Panel 2)			
1	CD3	UCHT1	eFluor 450	48-0038-42	Thermofisher
2	CD19	HIB19	eFluor 506	69-0199-42	Thermofisher
3	CD4	SK3	Super Bright 600	63-0047-42	Thermofisher
4	CD8a	SK1	PerCP-eFluor 710	46-0087-42	Thermofisher
5	CD38	HIT2	PE-eFluor 610	61-0389-42	Thermofisher
6	CD27	O323	Alexa Fluor700	56-0279-42	Thermofisher
7	CXCR5 (CD185)	MU5UBEE	FITC	11-9185-42	Thermofisher
8	ICOS (CD278)	C398.4A	PE	12-9949-81	Thermofisher
9	PD-1 (CD279)	eBioJ105 (J105)	PE-Cy7	25-2799-42	Thermofisher

10	HLA-DR	L243	Alexa Fluor647	A51010	Thermofisher
		Cytotoxic potential			
1	CD4	SK3	SuperBright600	63-0047-42	Thermofisher
2	CD8	SK1	PerCP-eFluor710	46-0087-42	Thermofisher
3	CD19	HIB19	eFluor 506	69-0199-42	Thermofisher
4	CD38	HIT2	PE-eFluor 610	61-0389-42	Thermofisher
5	HLA-DR	L243	Alexa Fluor 647	A51010	Thermofisher
6	GZMA (IC)	CB9	PE	12-9177-42	Thermofisher
7	GZMB (IC)	GB11	Alexa Fluor 488	MA5-23639	Thermofisher
8	Perforin (IC)	dG9	PE-Cy7	12-9177-42	Thermofisher
		Other Flow reagents			
1	Ultracompensation bead			01-2222-42	Thermofisher
2	Live/Dead Fixable Near IR staining kit			L10119	Thermofisher
2	FOXP3/TRN FACTOR STAIN BUFFER SET			00-5523-00	Thermofisher
3	FLOW STAIN BUFFER SOLN			00-4222-57	Thermofisher
4	SB COMPLETE STAINING BUFFER			SB-4401-42	Thermofisher
5	DPBS			D8537	Sigma
6	Pancoll human			P04-601000	Pan Biotech

457
458 **^{1}H-NMR metabolomics**
459
460 To obtain PBMCs metabolites, PBMCs were suspended in an optimized solvent extraction
461 mixture of 9:1 (methanol: chloroform) as described elsewhere in detail[75] and extracted with a
462 focused ultrasound system (Covaris E220, Woburn, USA). The extraction solutions were
463 evaporated to dryness for 4 hours in a vacuum concentrator and afterwards pellets
464 resuspended with 45 µL in a 1 mM TSP containing deuterated phosphate buffer. After
465 centrifugation at 20,000 x g for 10 min to remove residual macromolecules, 40 µL of the clear
466 supernatant were transferred to 1.7 mm NMR tubes. Spectra were recorded on ultrashielded
467 600 MHz spectrometer (Bruker AVANCE III HD, Karlsruhe, Germany) with a triple resonance
468 1.7 mm room temperature probe. Spectra used for analysis were acquired with a 2h 55min
469 lasting CPMG pulse program. Metabolite annotation and quantification were done with
470 ChenomX NMR Suite 8.3.
471
472 **Statistical analysis**
473

Bar diagrams were prepared using GraphPad Prism 6.0. Data shown are means ± SD. FACS data were analysed using one-way analysis of variance (ANOVA) for multiple group comparisons (mild, moderate, convalescent and HC) in GraphPad Prism software. No matching or pairing was used. Assumed Gaussian distribution with equal standard deviations (SDs) for experimental design. The mean of each group was compared with the mean of every other group and Tukey's post-hoc tests for multiple comparisons were employed. P-value considered significantly less than 0.05 or equal. Metabolite concentrations from ^{1}H-NMR analysis were exported as comma-separated value spreadsheet file to MetaboAnalyst 4.0 software, normalized with probabilistic quantile normalization (PQN) and range scaled. Unsupervised principal component analysis (PCA), a dimensionality-reduction method was used for clustering of all metabolites (PC1 and PC2 only). Multiple groups comparison was performed using one way ANOVA. Multivariate data analysis techniques such as partial least squares analysis (PLSDA) and variable's importance in the PLSDA (VIP) score analysis were used to find the correlation among different metabolites and various groups. Hierarchical clustering of all the metabolites was measured and distance measurement was performed with Pearson r correlation coefficient.

Figure legends:

Fig. 1: Comparison of monocytes and NK cell percentage amongst study groups.

A. The stained PBMCs were gated on the monocyte population and $CD3^{+}CD19^{+}$ cells were excluded. Cell populations are displayed for CD16 and CD14 expression (upper FACS panel). One exemplary dot plot is shown per study group. The bar diagrams (lower panel) show the non-classical ($CD16^{+}CD14^{-}$), intermediate ($CD16^{+}CD14^{+}$) and classical ($CD16^{-}CD14^{+}$) monocytes. *P-value ≤0.05, **P-value ≤0.01 and ***P-value ≤0.001.
B. UMAP plot for different subsets of monocytes (non-classical, intermediate and classical monocytes; left UMAP plot) from all the samples. Group comparisons among HC, mild and moderate (right UMAP plot). Colour coded information is provided for either different subsets of monocyte populations or patient groups.
C. The stained PBMCs were gated on lymphocyte population and further excluded the $CD3^{+}CD19^{+}$ cells and examined for the CD56 and CD8 expression in HC, mild, moderate and convalescent (upper FACS panel). One exemplary dot plot is shown per study group. The bar diagram shows the $CD56^{+}CD8^{+}CD3^{-}CD19^{-}$ NK cells. *P-value ≤0.05.

Fig. 2: Increased B cells in mild and moderate patients and reduced $CD8^{+}$ cytotoxic T cells in mild and convalescent patients

A. The stained PBMCs were gated on lymphocyte population and examined for the CD19 and CD3 expression in HC, mild, moderate and convalescent (upper FACS panel). One exemplary dot plot is shown per study group. The bar diagram shows $CD3^{-}CD19^{+}$ B cells. *P-value ≤0.05, **P-value ≤0.01 and ***P-value ≤0.001.
B. The $CD19^{-}CD3^{+}$ lymphocytes were examined for $CD4^{+}$ and $CD8^{+}$ T marker expression. One exemplary dot plot is shown per study group. There was statistically significant difference among HC, mild, moderate and convalescent (upper FACS panel).

However, $CD8^+$ T cells were significantly reduced in outpatient and convalescent patients. *P-value ≤0.05.

Fig. 3: Decreased activation and cytotoxic functional protein expression of $CD8^+$ T cells in convalescent patients

A. $CD8^+$ T cells were examined for the expression of activation marker HLA-DR (upper FACS panel). One exemplary dot plot is shown per study group. The bar diagram (lower panel) shows that HLA-DR was a significantly lower on $CD8^+$ T cells in mild, moderate and convalescent COVID-19^+ patients compared with HC. *P-value ≤0.05.
B. $CD8^+$ T cells were examined for the expression of their cytotoxic potential using granzyme A and perforin expression using IC staining (upper FACS panel). One exemplary dot plot is shown per study group. There was a statistically significant difference among HC, mild, moderate and convalescent (upper FACS panel) for granzyme A. The bar diagram (lower panel) shows that perforin expression was significantly lower on $CD8^+$ T cells in convalescent COVID-19^+ patients compared with HC, though mild and moderate represent a lower expression of perforin, but it did not to a significant level. *P-value ≤0.05.

Fig. 4: Increased exhausted $CD8^+$ T cells in convalescent patients

A. Expression of activation marker CD38 on $CD8^+$ T cells (upper FACS panel). One exemplary dot plot is shown per study group. The bar diagram (lower panel) shows that CD38 expression was significantly higher on $CD8^+$ T cells in convalescent COVID-19^+ patients compared with HC. *P-value ≤0.05.

B. Expression of activation marker CD38 and PD-1 on $CD8^+$ T cells (upper FACS panel). One exemplary dot plot is shown per study group. The bar diagram (lower panel) shows that PD-1^+CD38^+ expression on was a significantly higher on $CD8^+$ T cells in convalescent COVID-19^+ patients compared with HC. **P-value ≤0.01.

Fig. 5: ^{1}H-NMR spectroscopy of PBMC extracts

A. Heatmap of featured metabolites' concentrations plotted with SARS-CoV-2 progression group clustering.
B. Principle component analysis (PCA) was performed to identify the clustering of two different groups. HC and convalescent COVID-19 patient samples cluster together while SARS-Co-2 infected mild and moderate patients cluster in a separate cluster with PC1: 90.7% and PC2: 2.6%.
C. Box plots for differentially abundantly present metabolites in the different group including HC, mild, moderate, and convalescent COVID-19 patient. *P-value ≤0.05, **P-value ≤0.01 and ***P-value ≤0.001.

Fig. 6: Pattern hunter plots provide an insight of close correlations with other metabolites during COVID-19 infection.

A. Variable Importance in Projection (VIP) scores for all metabolites in the four studied groups.
B. Pattern hunter plot for glucose.
C. Pattern hunter plot for lactate and fructose.

Suppl. Fig. 1: Total % counts of monocytes and lymphocytes from PBMCs of COVID-19 patients.

A. Fixed PBMCs samples ($1x10^6$ cells) were acquired on flow cytometry on 2-3 different days for the entire experiments. Total 200,000 cells were acquired by flow cytometry and gating was performed based on FSC and SSC parameters for lymphocytes, monocytes and dead cells as described earlier[76-78]. Gating strategy for T lymphocytes (CD3, CD4 and CD8) monocytes (CD14 and CD16)[44], NK cells (CD56) using FMO controls.
B. The bar graphs represent the % of lymphocytes and monocytes.

Suppl. Fig. 2: UMAP analysis of lymphocytes and monocytes cell populations.

A. UMAP pseudo-colour plot was derived from all the samples. All the FCS files (used only live-cell gated population; minimum cells per samples were 25,000) were concatenated from HC, mild and moderate patients (upper panel). Representation of lymphocytes and monocytes populations in UMAP plot (middle panel). Presentation of different lymphocytes subpopulations like $CD4^+$ T cells, $CD8^+$ T cells, B cells, NK cells, NKT cells and regulatory T cells (lower panel).
B. UMAP plot for overlaying of different groups.
C. UMAP plot for different subsets of monocytes.
D. UMAP plots for individual antibody (protein) expression on monocyte populations. Scale bar shows the expression level of protein expression on the cell clusters (blue - lowest and red highest expression; relative expression).

Suppl. Fig. 3: Kinetics of regulatory T cells is not affected significantly in mild, moderate and convalescent patients.

$Foxp3^+$ expression on $CD19^-CD3^+CD4^+CD45RA^-$ T cells to identify the regulatory T cells in HC, outpatient, outpatient and convalescent (upper FACS panel). There was a statistically significant difference among HC, mild, moderate and convalescent (upper FACS panel).

Suppl. Fig. 4: Metabolite analysis in COVID-19 patients.

A. Analysis of Variance (ANOVA) for multi-group comparisons.
B. Partial Least Squares Discriminant Analysis (PLS-DA) scores plot.
C. Hierarchical clustering of metabolites (distance measured with Pearson r correlation coefficient).
D. Boxplots for branched-chain amino acids valine and leucine.

Author's contributions:

YS: Overall study design and project coordination, flow cytometry experiments, data analysis and interpretation and initial metabolic sample preparation, funding generation, and writing the manuscript.
CT: Metabolites sample preparation, Processing of the sample on ^{1}H-NMR, data analysis, data interpretation and writing
MO: Metabolites sample preparation, Processing of the sample on ^{1}H-NMR
RF, NK: Provided patient materials, Isolation of PBMCs, Performed the experiments for flowcytometry in BSL-2 facility, flow data interpretations.

RB: Isolation of PBMCs from HC and sample preparation for flow cytometry.
SO, MS, NC, OR: Study design, providing research tools, funding generation, data interpretation and writing and amending the manuscript.

All the authors have seen the manuscript, substantially contributed and agreed to be co-author.

Acknowledgements:

We thank you all the patients who participated in this study and FACS core facility (Klinikum-Berg) for accessing the Flow cytometry for the experiments. We also thanks Jana Held and Andrea Kreidenweiss from Institute of Tropical Medicine, Tübingen university for their help with coordination with clinical Trials and proof-reading of the manuscript. We acknowledge support by Deutsche Forschungsgemeinschaft (DFG) and Open Access Publishing Fund of University of Tübingen.

Funding:

RB is supported by Deutsche Forschungsgemeinschaft (DFG Project no. 426724658). EKFS (MS), DFG (OR), Ferring Pharmaceutical (YS and MSS). To MSS the Margarete von Wrangell (MvW 31-7635.41/118/3) habilitation scholarship co-funded by the Ministry of Science, Research and the arts (MWK) of the state of Baden-Württemberg and by the European Social Funds. Funders have no role in the study design and data analysis. To RF the German Federal Ministry of Education and Research (BMBF) (BMBF-01KI2052) and the German Federal Ministry of Health (BMG) (BMG-ZMVI1-1520COR801).

Competing interests:

Authors declare no financial competing interests.

DECOI Consortia

The members of the Deutsche COVID-19 Omics Initiative (DeCOI) are Janine Altmüller, Angel Angelov, Robert Bals, Alexander Bartholomäus, Anke Becker, Daniela Bezdan, Ezio Bonifacio, Peer Bork, Nicolas Casadei, Thomas Clavel, Maria Colome-Tatche, Andreas Diefenbach, Alexander Dilthey, Nicole Fischer, Konrad Förstner, Sören Franzenburg, Julia-Stefanie Frick, Gisela Gabernet, Julien Gagneur, Tina Ganzenmüller, Marie Gauder, Alexander Goesmann, Siri Göpel, Adam Grundhoff, Torsten Hain, Andrè Heimbach, Michael Hummel, Thomas Iftner, Angelika Iftner, Stefan Janssen, Jörn Kalinowski, René Kallies, Birte Kehr, Andreas Keller, Sarah Kim-Hellmuth, Christoph Klein, Oliver Kohlbacher, Karl Köhrer, Michael Knop, Jan O. Korbel, Peter G Kremsner, Denise Kühnert, Ingo Kurth, Markus Landthaler, Yang Li, Kerstin Ludwig, Oliwia Makarewicz, Manja Marz, Alice McHardy, Christian Mertes, Sven Nahsen, Markus Nöthen, Francine Ntoumi, Peter Nürnberg, Uwe Ohler, Stephan Ossowski, Jörg Overmann, Silke Peter, Klaus Pfeffer, Anna R. Poetsch, Alfred Pühler, Nikolaus Rajewsky, Markus Ralser, Olaf Rieß, Stephan Ripke, Ulisses Nunes da Rocha, Philip Rosenstiel, Antoine-Emmanuel Saliba, Leif Erik Sander, Birgit Sawitzki, Philipp Schiffer, Wulf Scheider, Eva-Christina Schulte, Joachim L. Schultze, Alexander Sczyrba, Yogesh Singh, Michael Sonnabend, Oliver Stegle, Jens Stoye, Fabian Theis, Janne Vehreschild, Thirumalaisamy P Velavan, Jörg Vogel, Max von Kleist, Andreas Walker, Jörn

Walter, Dagmar Wieczorek, Sylke Winkler, John Ziebuhr, Simone Scheithauer, Hajo Grundmann, Jonathan Schmid-Burgk, Ulrike Protzer and Inti Alberto De La Rosa Velázquez.

References:

1 Zhu, N. *et al.* A Novel Coronavirus from Patients with Pneumonia in China, 2019. *N Engl J Med* **382**, 727-733, doi:10.1056/NEJMoa2001017 (2020).

2 Dashboard, J. C.-L. https://coronavirus.jhu.edu/map.html. (2020).

3 Dashboard, W. L. https://covid19.who.int. (2020).

4 Chang, L., Yan, Y. & Wang, L. Coronavirus Disease 2019: Coronaviruses and Blood Safety. *Transfus Med Rev*, doi:10.1016/j.tmrv.2020.02.003 (2020).

5 Lehner, N. J. M. P. J. How does SARS-CoV-2 cause COVID-19? *Science*, 510-511 (2020).

6 Liu, J. *et al.* Community Transmission of Severe Acute Respiratory Syndrome Coronavirus 2, Shenzhen, China, 2020. *Emerg Infect Dis* **26**, doi:10.3201/eid2606.200239 (2020).

7 Singhal, T. A Review of Coronavirus Disease-2019 (COVID-19). *Indian J Pediatr* **87**, 281-286, doi:10.1007/s12098-020-03263-6 (2020).

8 WHO. <WHO-2019-nCoV-Sci_Brief-Transmission_modes-2020.3-eng.pdf>. *WHO Report* (2020).

9 Rothe, C. *et al.* Transmission of 2019-nCoV Infection from an Asymptomatic Contact in Germany. *N Engl J Med* **382**, 970-971, doi:10.1056/NEJMc2001468 (2020).

10 Xu, Z. *et al.* Pathological findings of COVID-19 associated with acute respiratory distress syndrome. *The Lancet Respiratory Medicine* **8**, 420-422, doi:10.1016/s2213-2600(20)30076-x (2020).

11 Wei Huang, J. B., Michelle McNamara, Suraj Saksena, Marsha Hartman, Tariq Arshad, Scott J. Bornheimerand Maurice O'Gorman. Lymphocyte Subset Counts in COVID-19 Patients: A Meta-Analysis. doi:10.1002/cytoa.24172 (2020).

12 Chen, G. *et al.* Clinical and immunological features of severe and moderate coronavirus disease 2019. *J Clin Invest* **130**, 2620-2629, doi:10.1172/JCI137244 (2020).

13 Shi, Y. *et al.* COVID-19 infection: the perspectives on immune responses. *Cell Death Differ*, doi:10.1038/s41418-020-0530-3 (2020).

14 Daniela Weiskopf1, K. S. S., Matthijs P. Raadsen, Alba Grifoni, Nisreen M.A. Okba, Henrik Endeman, Johannes P.C. van den Akker, Richard Molenkamp, Marion P.G. Koopmans, Eric C.M. van Gorp, Bart L. Haagmans, Rik L. de Swart, Alessandro Sette, Rory D. de Vries. Phenotype and kinetics of SARS-CoV-2-specific T cells in COVID-19 patients with acute respiratory distress syndrome. *Science Immunology*, doi:10.1126/sciimmunol.abd2071 (2020). (2020).

15 Del Valle, D. M. *et al.* An inflammatory cytokine signature predicts COVID-19 severity and survival. *Nature Medicine*, doi:10.1038/s41591-020-1051-9 (2020).

16 NcA OANA dOcEA, A. T., DANA ALBULEScU, OANA CRISTEA, & OVIdIU ZLATIAN, M. V., STERGHIOS A. MOScHOS, dIMITRIS TSOUKALAS, MARINA GOUMENOU, NIKOLAOS dRAKOULIS, JOSEF M. dUMANOV, VIcTOR A. TUTELYAN, GENNAdII G. ONIScHENKO, MIcHAEL AScHNER, dEMETRIOS A. SPANdIdOS and dANIELA cALINA. A new threat from an old enemy: Re-emergence of coronavirus (Review). *INTERNATIONAL JOURNAL OF MOLEcULAR MEdIcINE* **45**, 1631-1643 (2020).

17 Ong, E. Z. *et al.* A Dynamic Immune Response Shapes COVID-19 Progression. *Cell Host Microbe* **27**, 879-882 e872, doi:10.1016/j.chom.2020.03.021 (2020).

712 18 Picchianti Diamanti, A., Rosado, M. M., Pioli, C., Sesti, G. & Lagana, B. Cytokine Release
713 Syndrome in COVID-19 Patients, A New Scenario for an Old Concern: The Fragile
714 Balance between Infections and Autoimmunity. *Int J Mol Sci* **21**,
715 doi:10.3390/ijms21093330 (2020).
716 19 Vabret, N. *et al.* Immunology of COVID-19: Current State of the Science. *Immunity* **52**,
717 910-941, doi:10.1016/j.immuni.2020.05.002 (2020).
718 20 Velavan, T. P. & Meyer, C. G. Mild versus severe COVID-19: Laboratory markers. *Int J*
719 *Infect Dis* **95**, 304-307, doi:10.1016/j.ijid.2020.04.061 (2020).
720 21 Wu, H. *et al.* Clinical and Immune Features of Hospitalized Pediatric Patients With
721 Coronavirus Disease 2019 (COVID-19) in Wuhan, China. *JAMA Netw Open* **3**,
722 e2010895, doi:10.1001/jamanetworkopen.2020.10895 (2020).
723 22 Du, S. Q. & Yuan, W. Mathematical modeling of interaction between innate and
724 adaptive immune responses in COVID-19 and implications for viral pathogenesis. *J*
725 *Med Virol*, doi:10.1002/jmv.25866 (2020).
726 23 Giamarellos-Bourboulis, E. J. *et al.* Complex Immune Dysregulation in COVID-19
727 Patients with Severe Respiratory Failure. *Cell Host Microbe* **27**, 992-1000 e1003,
728 doi:10.1016/j.chom.2020.04.009 (2020).
729 24 Braciale, T. J. & Hahn, Y. S. Immunity to viruses. *Immunol Rev* **255**, 5-12,
730 doi:10.1111/imr.12109 (2013).
731 25 McKechnie, J. L. & Blish, C. A. The Innate Immune System: Fighting on the Front Lines
732 or Fanning the Flames of COVID-19? *Cell Host Microbe* **27**, 863-869,
733 doi:10.1016/j.chom.2020.05.009 (2020).
734 26 Thevarajan, I. *et al.* Breadth of concomitant immune responses prior to patient
735 recovery: a case report of non-severe COVID-19. *Nature Medicine*,
736 doi:10.1038/s41591-020-0819-2 (2020).
737 27 Assis, R. R. d. *et al.* Analysis of SARS-CoV-2 Antibodies in COVID-19 Convalescent
738 Plasma using a Coronavirus Antigen Microarray
739 . *bioRxiv preprint doi: https://doi.org/10.1101/2020.04.15.043364.*,
740 doi:10.1101/2020.04.15.043364 (2020).
741 28 Cao, Y. *et al.* Potent Neutralizing Antibodies against SARS-CoV-2 Identified by High-
742 Throughput Single-Cell Sequencing of Convalescent Patients' B Cells. *Cell* **182**, 73-84
743 e16, doi:10.1016/j.cell.2020.05.025 (2020).
744 29 Qin, C. *et al.* Dysregulation of immune response in patients with COVID-19 in Wuhan,
745 China. *Clin Infect Dis*, doi:10.1093/cid/ciaa248 (2020).
746 30 Song, J. W. *et al.* Immunological and inflammatory profiles in mild and severe cases of
747 COVID-19. *Nat Commun* **11**, 3410, doi:10.1038/s41467-020-17240-2 (2020).
748 31 Channappanavar, R., Fett, C., Zhao, J., Meyerholz, D. K. & Perlman, S. Virus-specific
749 memory CD8 T cells provide substantial protection from lethal severe acute
750 respiratory syndrome coronavirus infection. *J Virol* **88**, 11034-11044,
751 doi:10.1128/JVI.01505-14 (2014).
752 32 Janice Oh, H. L., Ken-En Gan, S., Bertoletti, A. & Tan, Y. J. Understanding the T cell
753 immune response in SARS coronavirus infection. *Emerg Microbes Infect* **1**, e23,
754 doi:10.1038/emi.2012.26 (2012).
755 33 Bost, P. *et al.* Host-Viral Infection Maps Reveal Signatures of Severe COVID-19
756 Patients. *Cell*, doi:10.1016/j.cell.2020.05.006 (2020).

34 Gardinassi, L. G., Souza, C. O. S., Sales-Campos, H. & Fonseca, S. G. Immune and Metabolic Signatures of COVID-19 Revealed by Transcriptomics Data Reuse. *Frontiers in Immunology* **11**, doi:10.3389/fimmu.2020.01636 (2020).
35 Ayres, J. S. Immunometabolism of infections. *Nat Rev Immunol* **20**, 79-80, doi:10.1038/s41577-019-0266-9 (2020).
36 Thaker, S. K., Ch'ng, J. & Christofk, H. R. Viral hijacking of cellular metabolism. *BMC Biol* **17**, 59, doi:10.1186/s12915-019-0678-9 (2019).
37 Moreno-Altamirano, M. M. B., Kolstoe, S. E. & Sanchez-Garcia, F. J. Virus Control of Cell Metabolism for Replication and Evasion of Host Immune Responses. *Front Cell Infect Microbiol* **9**, 95, doi:10.3389/fcimb.2019.00095 (2019).
38 Gupta, S. S., Wang, J. & Chen, M. Metabolic Reprogramming in CD8+ T Cells During Acute Viral Infections. *Frontiers in Immunology* **11**, doi:10.3389/fimmu.2020.01013 (2020).
39 Shehata, H. M. *et al.* Sugar or Fat?-Metabolic Requirements for Immunity to Viral Infections. *Front Immunol* **8**, 1311, doi:10.3389/fimmu.2017.01311 (2017).
40 Pallett, L. J., Schmidt, N. & Schurich, A. T cell metabolism in chronic viral infection. *Clin Exp Immunol* **197**, 143-152, doi:10.1111/cei.13308 (2019).
41 Swamy, M. *et al.* Glucose and glutamine fuel protein O-GlcNAcylation to control T cell self-renewal and malignancy. *Nat Immunol* **17**, 712-720, doi:10.1038/ni.3439 (2016).
42 Liew, C. C., Ma, J., Tang, H. C., Zheng, R. & Dempsey, A. A. The peripheral blood transcriptome dynamically reflects system wide biology: a potential diagnostic tool. *J Lab Clin Med* **147**, 126-132, doi:10.1016/j.lab.2005.10.005 (2006).
43 Xiong, Y. *et al.* Transcriptomic characteristics of bronchoalveolar lavage fluid and peripheral blood mononuclear cells in COVID-19 patients. *Emerg Microbes Infect* **9**, 761-770, doi:10.1080/22221751.2020.1747363 (2020).
44 Wong, K. L. *et al.* The three human monocyte subsets: implications for health and disease. *Immunol Res* **53**, 41-57, doi:10.1007/s12026-012-8297-3 (2012).
45 McInnes, L., Healy, J., Saul, N. & Großberger, L. UMAP: Uniform Manifold Approximation and Projection. *Journal of Open Source Software* **3**, doi:10.21105/joss.00861 (2018).
46 Liu, J. *et al.* Longitudinal characteristics of lymphocyte responses and cytokine profiles in the peripheral blood of SARS-CoV-2 infected patients. *EBioMedicine* **55**, 102763, doi:10.1016/j.ebiom.2020.102763 (2020).
47 Wang, F. *et al.* Characteristics of peripheral lymphocyte subset alteration in COVID-19 pneumonia. *J Infect Dis*, doi:10.1093/infdis/jiaa150 (2020).
48 Wen, W. *et al.* Immune cell profiling of COVID-19 patients in the recovery stage by single-cell sequencing. *Cell Discov* **6**, 31, doi:10.1038/s41421-020-0168-9 (2020).
49 Zhang, D. *et al.* COVID-19 infection induces readily detectable morphological and inflammation-related phenotypic changes in peripheral blood monocytes, the severity of which correlate with patient outcome. *medRxiv preprint doi: https://doi.org/10.1101/2020.03.24.20042655.* , doi:10.1101/2020.03.24.20042655 (2020).
50 Silvin, A. *et al.* Elevated Calprotectin and Abnormal Myeloid Cell Subsets Discriminate Severe from Mild COVID-19. *Cell*, doi:10.1016/j.cell.2020.08.002 (2020).
51 Takahashi, T. *et al.* Sex differences in immune responses that underlie COVID-19 disease outcomes. *Nature*, doi:10.1038/s41586-020-2700-3 (2020).

52 Jiang, Y. *et al.* COVID-19 pneumonia: CD8(+) T and NK cells are decreased in number but compensatory increased in cytotoxic potential. *Clin Immunol* **218**, 108516, doi:10.1016/j.clim.2020.108516 (2020).

53 Christopher Maucourant, I. F., Andrea Ponzetta, Soo Aleman, Martin Cornillet, Laura Hertwig Benedikt Strunz, Antonio Lentini, Björn Reinius, Demi Brownlie, Angelica Cuapio Gomez, Eivind Heggernes Ask, Ryan M. Hull, Alvaro Haroun-Izquierdo, Marie Schaffer, Jonas Klingström, Elin Folkesson, Marcus Buggert, Johan K. Sandberg, Lars I. Eriksson, Olav Rooyackers, Hans-Gustaf Ljunggren, Karl-Johan Malmberg, Jakob Michaëlsson, Nicole Marquardt, Quirin Hammer, Kristoffer Strålin, Niklas K. Björkström; and the Karolinska COVID-19 Study Group. Natural killer cell immunotypes related to COVID-19 disease severity. *Science Immunology*, doi:10.1126/sciimmunol.abd6832 (2020). (2020).

54 Diao, B. *et al.* Reduction and Functional Exhaustion of T Cells in Patients With Coronavirus Disease 2019 (COVID-19). *Front Immunol* **11**, 827, doi:10.3389/fimmu.2020.00827 (2020).

55 Katsuyama, E. *et al.* The CD38/NAD/SIRTUIN1/EZH2 Axis Mitigates Cytotoxic CD8 T Cell Function and Identifies Patients with SLE Prone to Infections. *Cell Rep* **30**, 112-123 e114, doi:10.1016/j.celrep.2019.12.014 (2020).

56 Zheng, H. Y. *et al.* Elevated exhaustion levels and reduced functional diversity of T cells in peripheral blood may predict severe progression in COVID-19 patients. *Cell Mol Immunol*, doi:10.1038/s41423-020-0401-3 (2020).

57 Zhou, R. *et al.* Acute SARS-CoV-2 Infection Impairs Dendritic Cell and T Cell Responses. *Immunity*, doi:10.1016/j.immuni.2020.07.026 (2020).

58 De Biasi, S. *et al.* Marked T cell activation, senescence, exhaustion and skewing towards TH17 in patients with COVID-19 pneumonia. *Nat Commun* **11**, 3434, doi:10.1038/s41467-020-17292-4 (2020).

59 Francisco, L. M., Sage, P. T. & Sharpe, A. H. The PD-1 pathway in tolerance and autoimmunity. *Immunol Rev* **236**, 219-242, doi:10.1111/j.1600-065X.2010.00923.x (2010).

60 Zhang, J. Y. *et al.* Single-cell landscape of immunological responses in patients with COVID-19. *Nat Immunol* **21**, 1107-1118, doi:10.1038/s41590-020-0762-x (2020).

61 Westmeier, J. *et al.* Impaired Cytotoxic CD8(+) T Cell Response in Elderly COVID-19 Patients. *mBio* **11**, doi:10.1128/mBio.02243-20 (2020).

62 Mazzoni, A. *et al.* Impaired immune cell cytotoxicity in severe COVID-19 is IL-6 dependent. *J Clin Invest*, doi:10.1172/JCI138554 (2020).

63 Kusnadi, A. *et al.* Severely ill COVID-19 patients display impaired exhaustion features in SARS-CoV-2-reactive CD8(+) T cells. *Sci Immunol* **6**, doi:10.1126/sciimmunol.abe4782 (2021).

64 Cabrera-Marante, O. *et al.* Perforin gene variant A91V in young patients with severe COVID-19. *Haematologica* **105**, 2844-2846, doi:10.3324/haematol.2020.260307 (2020).

65 Zeng, Y. *et al.* Peripheral Blood Mononuclear Cell Metabolism Acutely Adapted to Postprandial Transition and Mainly Reflected Metabolic Adipose Tissue Adaptations to a High-Fat Diet in Minipigs. *Nutrients* **10**, doi:10.3390/nu10111816 (2018).

66 Codo, A. C. *et al.* Elevated Glucose Levels Favor SARS-CoV-2 Infection and Monocyte Response through a HIF-1alpha/Glycolysis-Dependent Axis. *Cell Metab*, doi:10.1016/j.cmet.2020.07.007 (2020).

850 67 Jaiswal, N., Agrawal, S. & Agrawal, A. High fructose-induced metabolic changes
851 enhance inflammation in human dendritic cells. *Clin Exp Immunol* **197**, 237-249,
852 doi:10.1111/cei.13299 (2019).
853 68 Di Wu, T. S., Xiaobo Yang, Jian-Xin Song Mingliang Zhang Chengye Yao Wen Liu, Muhan
854 Huang, Yuan Yu, Qingyu Yang Tingju Zhu, Jiqian Xu, Jingfang Mu, Yaxin Wang, Hong
855 Wang, Tang Tang, Yujie Ren Yongran Wu, Shu-Hai Lin, Yang Qiu, Ding-Yu Zhang, You
856 Shang, Xi Zhou. Plasma Metabolomic and Lipidomic Alterations Associated with
857 COVID-19. *Natl Sci Rev*, doi:10.1093/nsr/nwaa086 (2020).
858 69 Ferrara, F., De Rosa, F. & Vitiello, A. The Central Role of Clinical Nutrition in COVID-19
859 Patients During and After Hospitalization in Intensive Care Unit. *SN Compr Clin Med*,
860 1-5, doi:10.1007/s42399-020-00410-0 (2020).
861 70 Ferreira, C. *et al.* Non-obese diabetic mice select a low-diversity repertoire of natural
862 regulatory T cells. *Proc Natl Acad Sci U S A* **106**, 8320-8325,
863 doi:10.1073/pnas.0808493106 (2009).
864 71 Watford, M. Glutamine and glutamate: Nonessential or essential amino acids? *Anim*
865 *Nutr* **1**, 119-122, doi:10.1016/j.aninu.2015.08.008 (2015).
866 72 Max W. S. Oliveira, J. B. M., Marcos R. de Oliveira, Alfeu Zanotto-Filho, Guilherme A.
867 Behr, Ricardo F. Rocha, José C. F. Moreira, Fábio Klamt. Scavenging and antioxidant
868 potential of physiological taurine concentrations against different reactive
869 oxygen/nitrogen species
870 . *Pharmaceutical Reports* **62**, 185-193 (2010).
871 73 Cunningham, L., Simmonds, P., Kimber, I., Basketter, D. A. & McFadden, J. P. Perforin
872 and resistance to SARS coronavirus 2. *J Allergy Clin Immunol* **146**, 52-53,
873 doi:10.1016/j.jaci.2020.05.007 (2020).
874 74 Maskus, D. J. *et al.* Characterization of a novel inhibitory human monoclonal antibody
875 directed against Plasmodium falciparum Apical Membrane Antigen 1. *Sci Rep* **6**, 39462,
876 doi:10.1038/srep39462 (2016).
877 75 Lorenz, M. A., Burant, C. F. & Kennedy, R. T. Reducing time and increasing sensitivity
878 in sample preparation for adherent mammalian cell metabolomics. *Anal Chem* **83**,
879 3406-3414, doi:10.1021/ac103313x (2011).
880 76 Marimuthu, R. *et al.* Characterization of Human Monocyte Subsets by Whole Blood
881 Flow Cytometry Analysis. *J Vis Exp*, doi:10.3791/57941 (2018).
882 77 Autissier, P., Soulas, C., Burdo, T. H. & Williams, K. C. Evaluation of a 12-color flow
883 cytometry panel to study lymphocyte, monocyte, and dendritic cell subsets in humans.
884 *Cytometry A* **77**, 410-419, doi:10.1002/cyto.a.20859 (2010).
885 78 Davies, R., Vogelsang, P., Jonsson, R. & Appel, S. An optimized multiplex flow
886 cytometry protocol for the analysis of intracellular signaling in peripheral blood
887 mononuclear cells. *J Immunol Methods* **436**, 58-63, doi:10.1016/j.jim.2016.06.007
888 (2016).
889

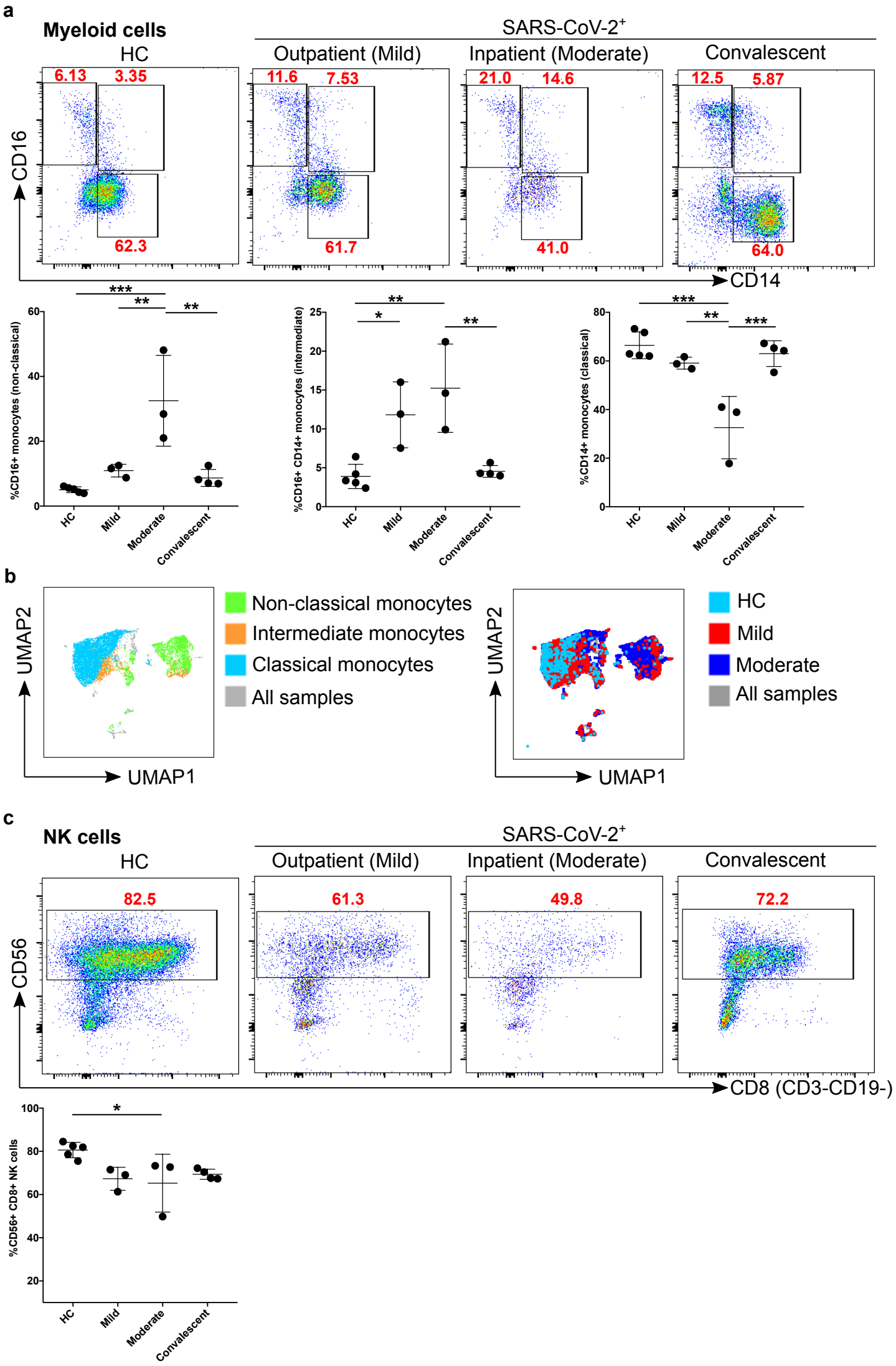
a
Myeloid cells
SARS-CoV-2+
HC
Outpatient (Mild)
Inpatient (Moderate)
Convalescent
6.13
3.35
62.3
11.6
7.53
61.7
21.0
14.6
41.0
12.5
5.87
64.0
CD16
CD14
%CD16+ monocytes (non-classical)
%CD16+ CD14+ monocytes (intermediate)
%CD14+ monocytes (classical)
HC
Mild
Moderate
Convalescent
b
UMAP2
UMAP1
Non-classical monocytes
Intermediate monocytes
Classical monocytes
All samples
HC
Mild
Moderate
All samples
c
NK cells
SARS-CoV-2+
HC
Outpatient (Mild)
Inpatient (Moderate)
Convalescent
82.5
61.3
49.8
72.2
CD56
CD8 (CD3-CD19-)
%CD56+ CD8+ NK cells
HC
Mild
Moderate
Convalescent

Fig. 1

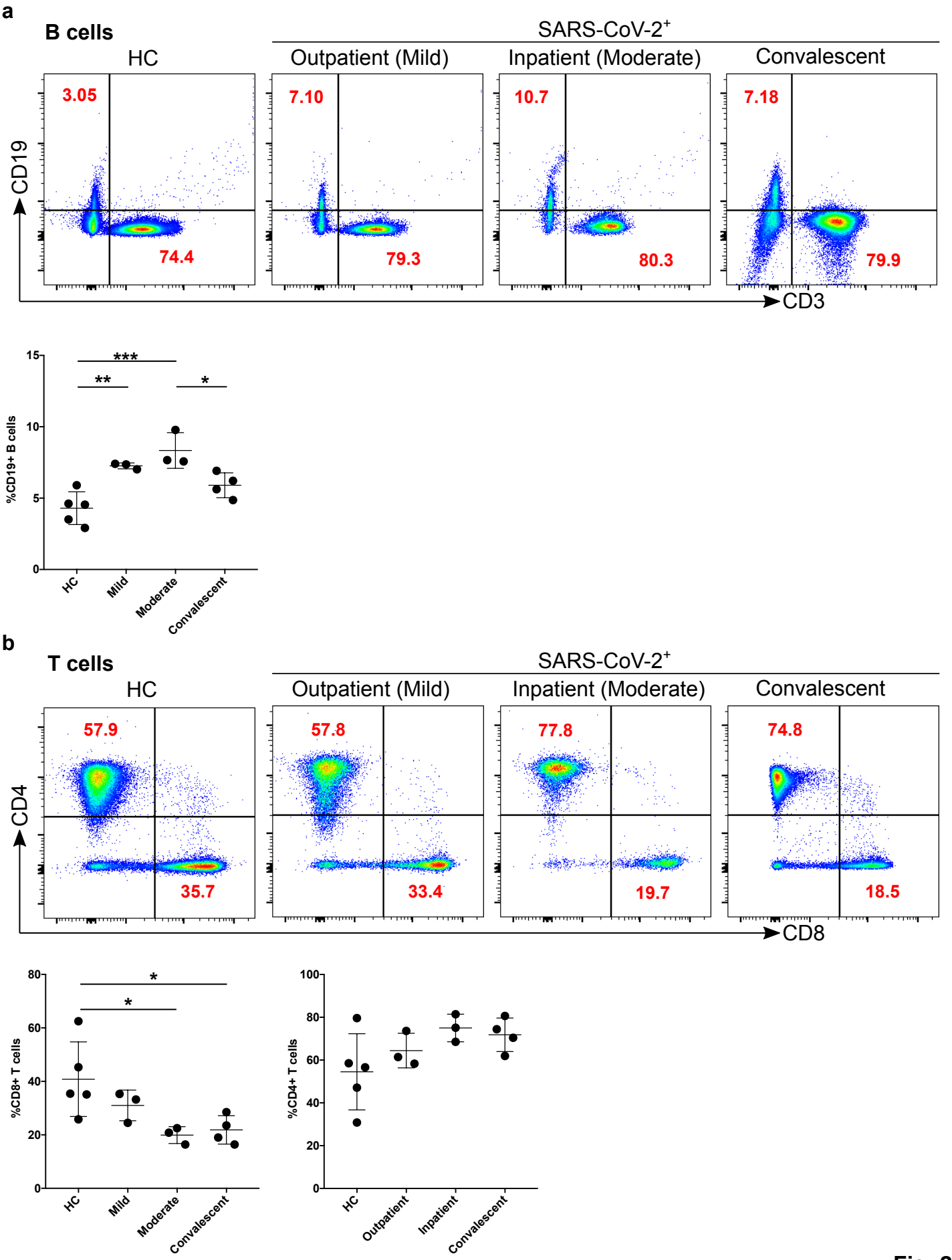
a
B cells
SARS-CoV-2+
HC
Outpatient (Mild)
Inpatient (Moderate)
Convalescent
3.05
74.4
7.10
79.3
10.7
80.3
7.18
79.9
CD19
CD3
%CD19+ B cells
***
**
*
HC
Mild
Moderate
Convalescent
b
T cells
SARS-CoV-2+
HC
Outpatient (Mild)
Inpatient (Moderate)
Convalescent
57.9
35.7
57.8
33.4
77.8
19.7
74.8
18.5
CD4
CD8
%CD8+ T cells
%CD4+ T cells
HC
Mild
Moderate
Convalescent
Outpatient
Inpatient

Fig. 2

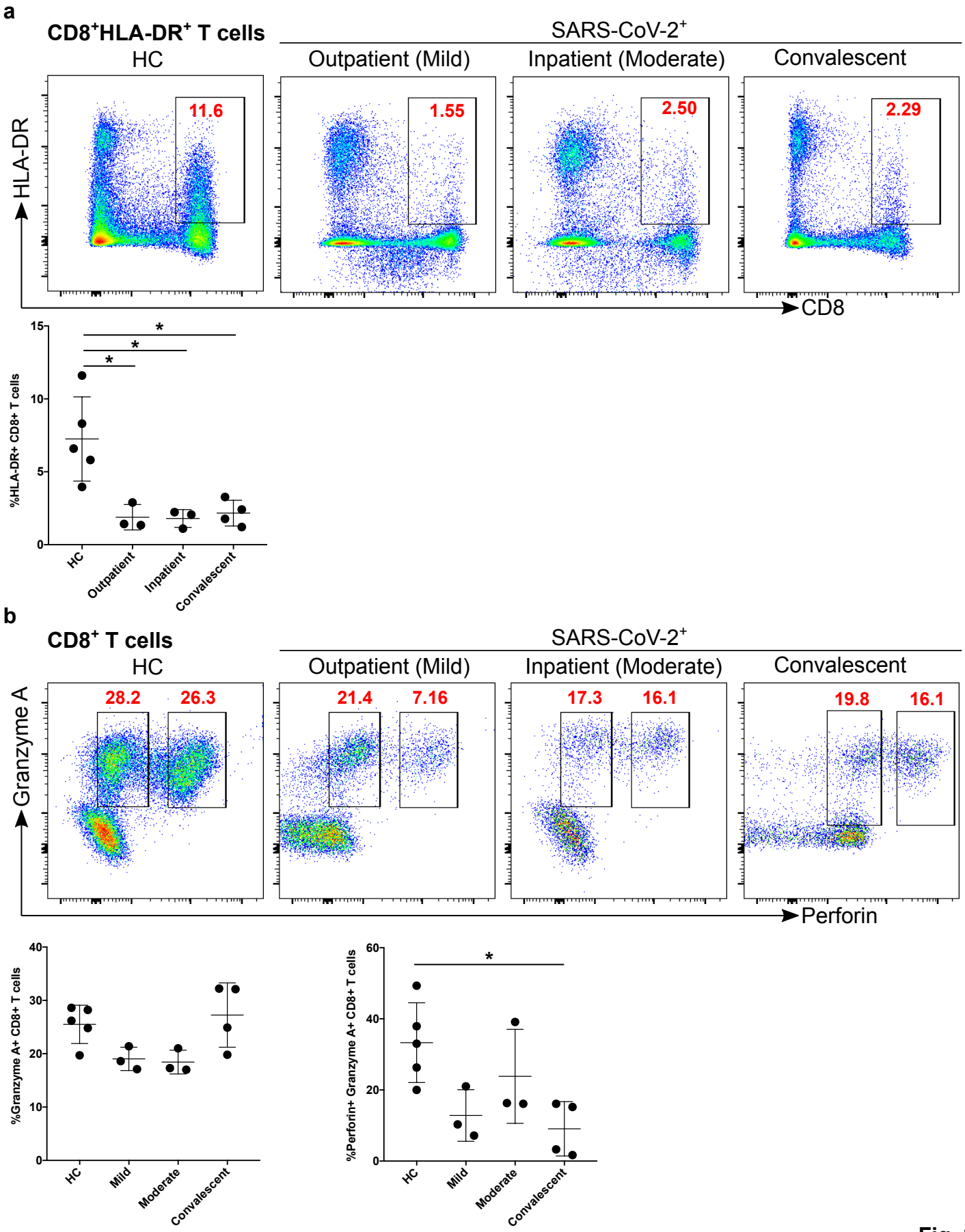
a
CD8+HLA-DR+ T cells
SARS-CoV-2+
HC
Outpatient (Mild)
Inpatient (Moderate)
Convalescent
11.6
1.55
2.50
2.29
HLA-DR
CD8
%HLA-DR+ CD8+ T cells
HC
Outpatient
Inpatient
Convalescent
b
CD8+ T cells
SARS-CoV-2+
HC
Outpatient (Mild)
Inpatient (Moderate)
Convalescent
28.2
26.3
21.4
7.16
17.3
16.1
19.8
16.1
Granzyme A
Perforin
%Granzyme A+ CD8+ T cells
%Perforin+ Granzyme A+ CD8+ T cells
HC
Mild
Moderate
Convalescent

Fig. 3

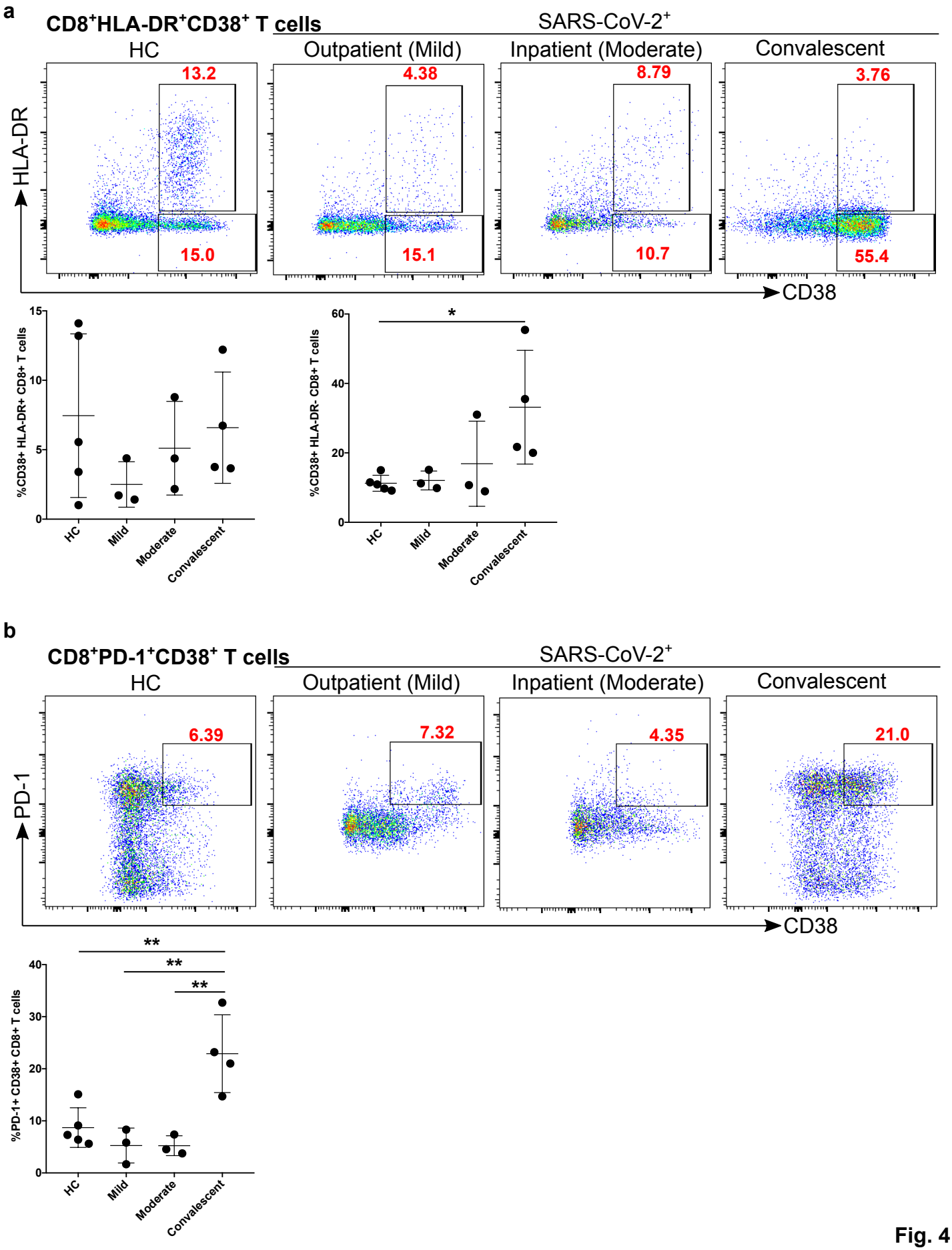
a
CD8+HLA-DR+CD38+ T cells
SARS-CoV-2+
HC
Outpatient (Mild)
Inpatient (Moderate)
Convalescent
13.2
15.0
4.38
15.1
8.79
10.7
3.76
55.4
HLA-DR
CD38
%CD38+ HLA-DR+ CD8+ T cells
%CD38+ HLA-DR- CD8+ T cells
*
HC
Mild
Moderate
Convalescent
b
CD8+PD-1+CD38+ T cells
SARS-CoV-2+
HC
Outpatient (Mild)
Inpatient (Moderate)
Convalescent
6.39
7.32
4.35
21.0
PD-1
CD38
%PD-1+ CD38+ CD8+ T cells
**
**
**
HC
Mild
Moderate
Convalescent

Fig. 4

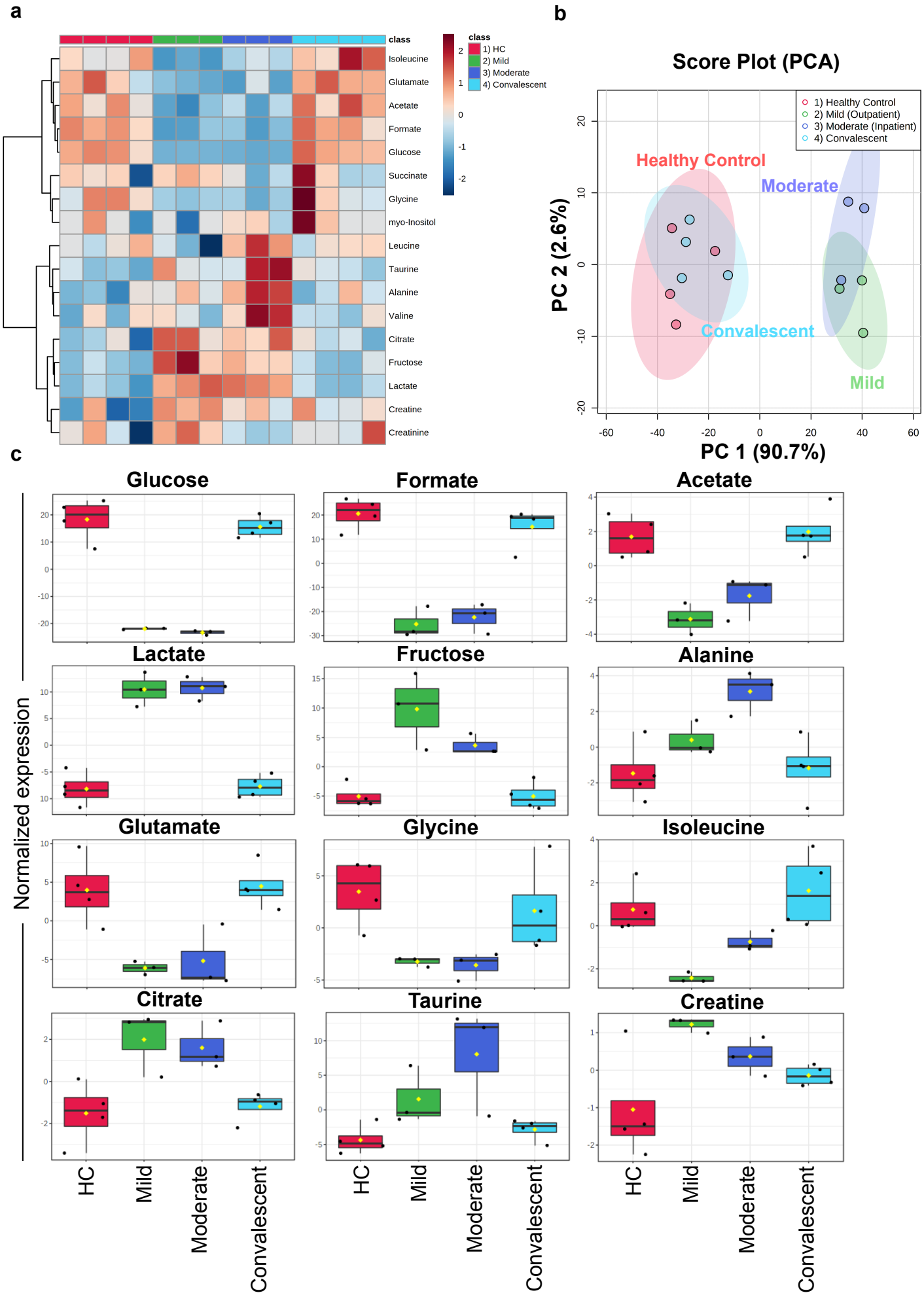
a
class
1) HC
2) Mild
3) Moderate
4) Convalescent
Isoleucine
Glutamate
Acetate
Formate
Glucose
Succinate
Glycine
myo-Inositol
Leucine
Taurine
Alanine
Valine
Citrate
Fructose
Lactate
Creatine
Creatinine
b
Score Plot (PCA)
1) Healthy Control
2) Mild (Outpatient)
3) Moderate (Inpatient)
4) Convalescent
Healthy Control
Moderate
Convalescent
Mild
PC 2 (2.6%)
PC 1 (90.7%)
c
Glucose
Formate
Acetate
Lactate
Fructose
Alanine
Glutamate
Glycine
Isoleucine
Citrate
Taurine
Creatine
Normalized expression
HC
Mild
Moderate
Convalescent

Fig. 5

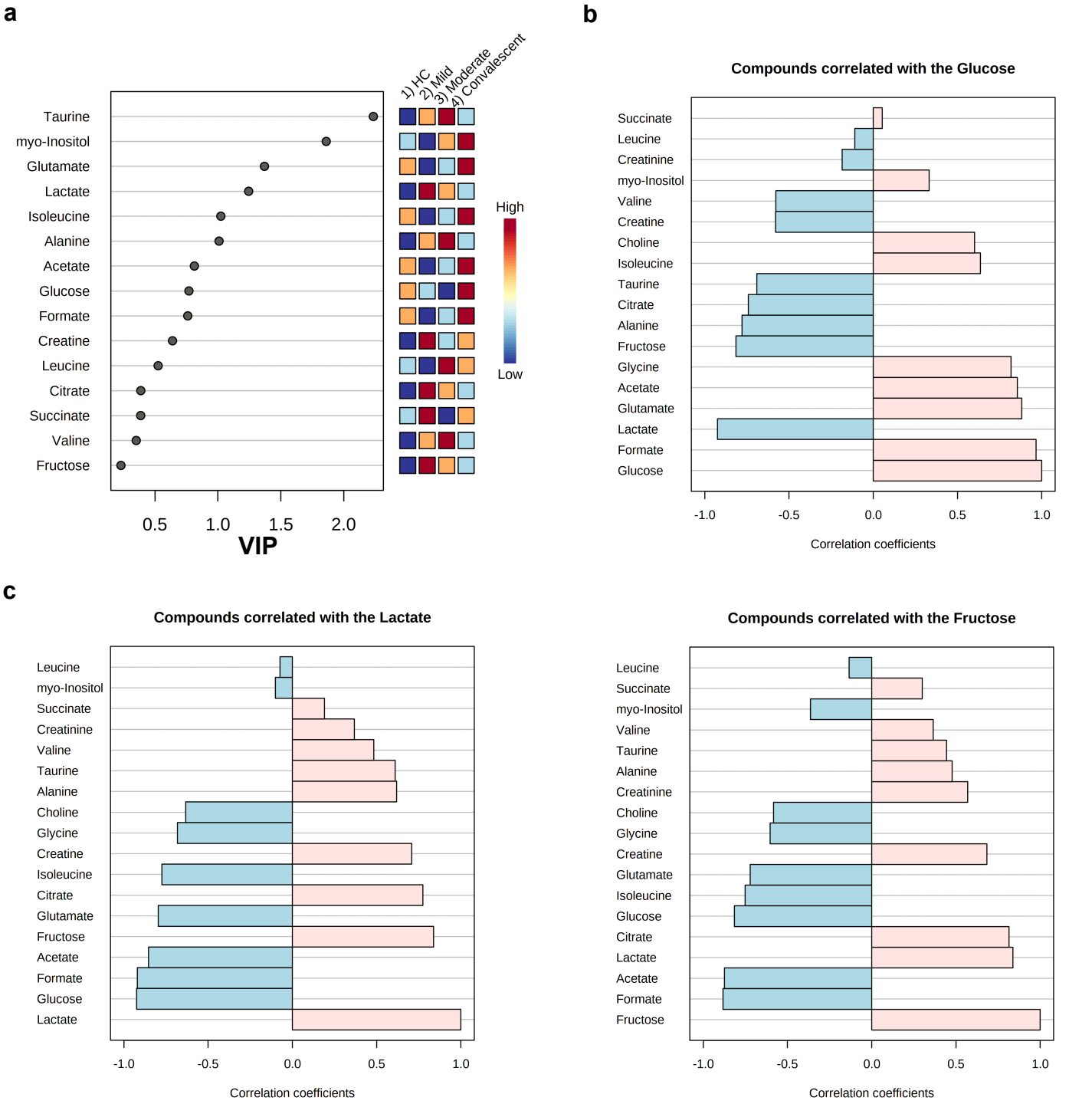
a
1) HC
2) Mild
3) Moderate
4) Convalescent
Taurine
myo-Inositol
Glutamate
Lactate
Isoleucine
Alanine
Acetate
Glucose
Formate
Creatine
Leucine
Citrate
Succinate
Valine
Fructose
High
Low
0.5
1.0
1.5
2.0
VIP
b
Compounds correlated with the Glucose
Succinate
Leucine
Creatinine
myo-Inositol
Valine
Creatine
Choline
Isoleucine
Taurine
Citrate
Alanine
Fructose
Glycine
Acetate
Glutamate
Lactate
Formate
Glucose
-1.0
-0.5
0.0
0.5
1.0
Correlation coefficients
c
Compounds correlated with the Lactate
Leucine
myo-Inositol
Succinate
Creatinine
Valine
Taurine
Alanine
Choline
Glycine
Creatine
Isoleucine
Citrate
Glutamate
Fructose
Acetate
Formate
Glucose
Lactate
-1.0
-0.5
0.0
0.5
1.0
Correlation coefficients
Compounds correlated with the Fructose
Leucine
Succinate
myo-Inositol
Valine
Taurine
Alanine
Creatinine
Choline
Glycine
Creatine
Glutamate
Isoleucine
Glucose
Citrate
Lactate
Acetate
Formate
Fructose
-1.0
-0.5
0.0
0.5
1.0
Correlation coefficients

Fig. 6